WATER RESOURCES RESEARCH, VOL. 37, NO. 10, PAGES 2607–2618, OCTOBER 2001

Stability of creeping soil and implications for hillslope evolution

David Jon Furbish

Department of Geological Sciences and Geophysical Fluid Dynamics Institute, Florida State University
Tallahassee, Florida

Sergio Fagherazzi

School of Computational Science and Information Technology, Florida State University, Tallahassee, Florida

Abstract. The geomorphic behavior of a soil-mantled hillslope undergoing diffusive creep involves a coupling between changes in land surface elevation, soil transport rates, soil production, and soil thickness. A linear stability analysis suggests that the coupled response of the soil mantle to small perturbations in soil thickness or surface topography is influenced by two factors. The diffusive-like behavior of soil creep has a stabilizing effect wherein perturbations in land surface elevation are damped. The relation between the soil production rate and soil thickness may be either stabilizing or destabilizing. A monotonically decreasing production rate with soil thickness reinforces the stabilizing effect of diffusive land surface smoothing. An increasing production rate with soil thickness has a destabilizing effect wherein perturbations in soil thickness or the soil-bedrock interface are amplified, despite the presence of diffusive land surface smoothing. This coupled behavior is insensitive to the transport relation, whether the soil flux is proportional to the land surface gradient or to the product of the soil thickness and land surface gradient. The latter type of relation, nonetheless, could lead to a more complex hillslope form than might otherwise be expected for purely diffusive transport. Moreover, the response to periodic (sinusoidal) variations in the rate of stream downcutting at the lower hillslope boundary involves upslope propagation of coupled (damped) waveforms in the land surface and the soil-bedrock interface. The distance of upslope propagation goes with the square root of the product of the transport diffusion-like coefficient and the period of the downcutting rate. The upper part of the hillslope is therefore insensitive to relatively high-frequency variations in stream downcutting, so together with a stable behavior of the coupled soil-mantle-bedrock system, this part of the hillslope may exhibit a tendency toward uniform lowering, while the lower part behaves transiently. Conversely, in the presence of low-frequency variations in stream downcutting, hillslope morphology and soil thickness variations are more likely to reflect unsteady conditions over the entirety of the hillslope.

1. Introduction

A longstanding premise in hillslope geomorphology holds that for soils developing on bedrock, changes in land surface geometry involve a coupling between the rate of soil transport, the rate of soil production by chemical and mechanical processes, and changes in soil thickness or bulk density. *Carson and Kirkby* [1972, p. 104–106], following ideas proposed by *Gilbert* [1877, 1909], clearly articulate the special role of soil production in this coupling, in particular, the significance of the form of the relation between the rate of soil production and soil thickness (Figure 1). Inasmuch as soil production mostly depends on weathering associated with circulation of water, *Carson and Kirkby* [1972] suggest that this relation ought to exhibit a maximum at an intermediate soil thickness. Then, for a given rate of erosion (or deposition), perturbations in thickness for soils to the right of the maximum are damped (a stable behavior), whereas perturbations in thickness for soils to the left of the maximum grow unstably. Note, however, that this qualitative description of soil thickness stability is only loosely related to transport rates; the question remains how perturbations in soil thickness (or land surface elevation) modify transport rates which, via a feedback process, alter soil thickness and production. Because transport rates generally depend on land surface geometry and because changes in land surface elevation generally involve a divergence of transport rates, a full characterization of the feedback between land surface geometry, soil transport, soil thickness, and soil production must be obtained within the context of a specific model that fully couples these four elements.

Toward this end, key ingredients of a fully coupled model are currently in place for the case of soil-mantled hillslopes undergoing diffusive creep. Specifically, there is a long record of work suggesting that at scales larger than local roughening processes [e.g., *Jyotsna and Haff*, 1997] such hillslopes evolve according to a diffusion-like equation [e.g., *Culling*, 1963, 1965; *Kirkby*, 1967; *Carson and Kirkby*, 1972; *Hirano*, 1975; *Bucknam and Anderson*, 1979; *Nash*, 1980a, 1980b; *McKean et al*., 1993; *Dietrich et al*., 1995; *Fernandes and Dietrich*, 1997; *Heimsath et al*., 1999]. More recently, field measurements involving cosmogenic isotopes provide clear evidence that the rate of soil production can be described as a monotonically decreasing function of soil thickness in the presence of biomechanically

Paper number 2001WR000239.
0043-1397/01/2001WR000239$09.00

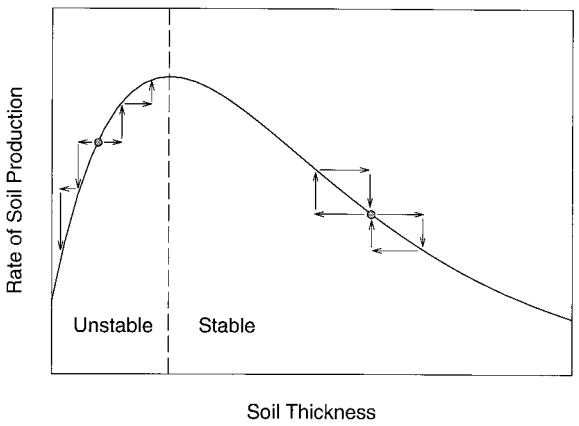

Figure 1. Schematic diagram of soil production rate versus soil thickness showing stable and unstable responses of initial states (circles) to perturbations in soil thickness, modified from Figure 5.5 of *Carson and Kirkby* [1972, p. 105].

driven creep [e.g., *Heimsath et al*., 1997, 1999], a result that is qualitatively consistent with that part of the curve to the right of the maximum in Figure 1. Taken together, these ingredients provide necessary and sufficient conditions to formally characterize the coupling between land surface geometry, soil transport, soil thickness, and soil production.

A concise way to characterize this coupling is provided by the formal framework of a linear stability analysis of a creeping soil mantle. The basic idea of the analysis is this: The analysis starts with a description of hillslope geometry compatible with a specified, uniform soil thickness and a steady, uniform rate of land surface lowering [e.g., *Fernandes and Dietrich*, 1997]. This defines a basic state for the hillslope-soil-mantle system. The analysis then "poses" the following: Suppose this basic state is disturbed; that is, variations in land surface elevation or soil thickness (or both) having the form of two-dimensional swales or convexities are imposed on the basic state. Does the coupling between land surface geometry, soil transport, soil thickness, and soil production respond unstably by amplifying these features, or does it respond in a stable manner by attenuating them? The analysis then clarifies the specific physical and geometrical conditions, the initial soil thickness, soil production rate, and size of disturbance, under which these alternative responses occur, and it clarifies, for given conditions, the relative rate of response. In a mathematical sense the analysis formally pertains to infinitesimal-amplitude disturbances. That is, it leaves open the possibility that a system predicted to be stable for small disturbances may be unstable with large disturbances. Conversely, the behavior of a system predicted to be unstable for small-amplitude disturbances does not necessarily involve unbounded amplification of these features, as additional factors may influence their behavior as they grow to "finite amplitude."

In pursuing this stability analysis, we consider two formulations for soil transport. The first assumes that the soil flux is proportional to the land surface gradient, a formulation that is most conventionally adopted, albeit possibly a special case of a more general nonlinear relation [e.g., *Roering et al*., 1999]. The second assumes that the soil flux is proportional to the product of soil thickness and land surface gradient, an idea first proposed by *Ahnert* [1967] and examined recently by *Furbish and Dietrich* [1999, 2000], *Braun et al*. [2000], and W. E. Dietrich and D. J. Furbish (On the use of a diffusion-like equation to describe hillslope evolution, 2, Slope-dependent transport and the diffusion coefficient, manuscript in preparation, 2001) (hereinafter referred to as Dietrich and Furbish, manuscript in preparation, 2001). In addition, we consider a general relation for the rate of soil production which mimics that in Figure 1 and which reduces as a special case to the exponential function described by *Heimsath et al*. [1997, 1999].

The analysis suggests that a soil mantle on a hillslope undergoing creep responds to small perturbations in soil thickness and surface topography in a manner similar to that envisioned by *Carson and Kirkby* [1972] (Figure 1). Two factors influence this behavior. The diffusive-like behavior of soil creep, because it tends to smooth topographic irregularities, has a universally stabilizing effect wherein perturbations in land surface elevation are damped. The relation between the soil production rate and soil thickness may be either stabilizing or destabilizing. A decreasing production rate with soil thickness (to the right of the maximum in Figure 1) reinforces the stabilizing effect of diffusive land surface smoothing. However, an increasing production rate with soil thickness (to the left of the maximum in Figure 1) has a destabilizing effect wherein perturbations in soil thickness or the soil-bedrock interface are amplified, despite the presence of diffusive land surface smoothing.

Our results reinforce previous suggestions that there is a need to more fully understand detailed effects of boundary conditions at the base of a hillslope [e.g., *Armstrong*, 1987; *Fernandes and Dietrich*, 1997], as these conditions influence the long-term response of the hillslope to disturbances in soil thickness and surface topography. In particular, we illustrate how the response to periodic variations in downcutting rate involves upslope propagation of coupled (damped) waveforms in the land surface and the soil-bedrock interface. Because the system is highly dissipative, only low-frequency variations in downcutting rate and associated waveforms influence the upper part of the hillslope. The insensitivity of this part of the hillslope to relatively high-frequency variations at the lower boundary, together with a stable behavior of the coupled soil-mantle-bedrock system, suggests that the upper part of the hillslope may exhibit a tendency toward uniform lowering as envisioned by *Gilbert* [1877, 1909], while the lower part behaves transiently. Conversely, in the presence of low-frequency variations in stream downcutting, hillslope morphology and soil thickness variations are more likely to reflect unsteady conditions over the entirety of the hillslope. We also demonstrate that if the soil flux is proportional to the product of soil thickness and land surface gradient and if the rate of soil production, for given soil thickness, increases with downslope distance for hydrogeochemical reasons, then it is entirely conceivable to have a convex-concave hillslope profile with a steady, uniform rate of land surface lowering, a situation that is not normally attributed to purely diffusive transport.

2. Model of Hillslope Evolution by Soil Creep

Consider a Cartesian *xyz* coordinate system associated with a hillslope (Figure 2). The horizontal x axis is positive in the downslope direction with origin ($x = 0$) at the hillslope crest. The base of the hillslope is positioned at $x = X$. The horizontal y axis is positive toward the left when looking downslope, with origin ($y = 0$) along the hillslope "axis." For later reference a convenient hillslope "width" b is defined by $y = \pm b/2$. The z axis is positive upward. Let $z = \zeta$ denote the local position of the land surface and let $z = \eta$ denote the local

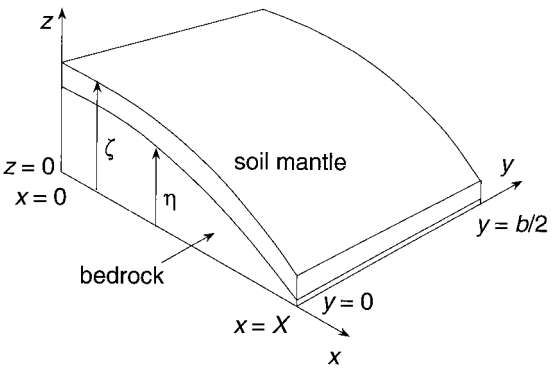

Figure 2. Definition diagram of coordinate system adopted for soil-mantled hillslope.

position of the base of the active soil. By definition, the active soil thickness $h = \zeta - \eta$.

An appropriate depth-integrated equation of conservation of mass is [*Furbish and Dietrich*, 1999; see also *Heimsath et al*., 1999; D. J. Furbish and W. E. Dietrich, On the use of a diffusion-like equation to describe hillslope evolution, 1, Formulation and scaling, manuscript in preparation, 2001 (hereinafter referred to as Furbish and Dietrich, manuscript in preparation)]

$$\nabla_2 \cdot (h\mathbf{q}) + \frac{\partial}{\partial t}(hc_h) + c_\eta \frac{\partial \eta}{\partial t} = 0, \tag{1}$$

where $\nabla_2 = \mathbf{i}\partial/\partial x + \mathbf{j}\partial/\partial y$, $\mathbf{q} = \mathbf{i}q_x + \mathbf{j}q_y$ $[L\ t^{-1}]$ is the depth-averaged, volumetric soil flux density, c_h is the vertically averaged soil concentration, and c_η is the concentration at the base of the soil ($z = \eta$). (By definition, the concentration $c = 1 - n$, where n is the soil porosity.)

Several phenomenological relations have been proposed to describe the depth-integrated volumetric flux $h\mathbf{q}$ $[L^2\ t^{-1}]$ for soil creep. It is conventionally assumed that this flux satisfies a relation of the form

$$h\mathbf{q} = -D_V \nabla_2 \zeta, \tag{2}$$

where D_V $[L^2\ t^{-1}]$ is a diffusion-like coefficient. An analysis of the time-averaged creep rate data provided by *McKean et al*. [1993] alternatively suggests the possibility that the depth-averaged flux density is proportional to slope [*Furbish and Dietrich*, 1999, 2000; Dietrich and Furbish, manuscript in preparation, 2001]; namely,

$$\mathbf{q} = -D\nabla_2 \zeta, \tag{3}$$

where $D = D_V/h$ $[L\ t^{-1}]$ is a quasi-local transport coefficient. In this formulation the depth-integrated flux $h\mathbf{q}$ is proportional to the depth-slope product, an idea suggested by *Ahnert* [1967].

Using $\zeta = \eta + h$, substitution of (2) into (1) then leads to

$$\nabla_2 \cdot [D_V \nabla_2 (\eta + h)] - \frac{\partial}{\partial t}(hc_h) - c_\eta \frac{\partial \eta}{\partial t} = 0, \tag{4}$$

whereas using (3),

$$\nabla_2 \cdot [Dh\nabla_2 (\eta + h)] - \frac{\partial}{\partial t}(hc_h) - c_\eta \frac{\partial \eta}{\partial t} = 0. \tag{5}$$

Field measurements involving cosmogenic isotopes further suggest that the rate of soil production varies with soil thickness [e.g., *Heimsath et al*., 1997, 1999]; namely,

$$\frac{\partial \eta}{\partial t} = -W_0 e^{-h/\gamma}, \tag{6}$$

where W_0 is a nominal rate of soil production when $h \to 0$ and γ is a length scale that characterizes the rate of decline in the soil production rate with increasing soil thickness. Here soil production is envisioned as being largely a mechanical process wherein biogenic activity plays a dominant role in mechanically disrupting the underlying bedrock, albeit in concert with chemical weathering and possibly other mechanisms [*Heimsath et al*., 1999, pp. 153–154]. Note that the essence of (6) is to characterize a stabilizing, negative feedback mechanism, consistent with that part of the curve to the right of the maximum in Figure 1.

On heuristic grounds we generalize (6) to

$$\frac{\partial \eta}{\partial t} = -W_0 \left(\frac{1 + \kappa h}{1 + \kappa \gamma} \right) e^{-h/\gamma}, \tag{7}$$

which describes a curve having the form of that in Figure 1 while retaining the essence of (6). Here $\kappa[L^{-1}]$ is a coefficient that modulates the intercept and the rate of increase in the soil production rate with increasing soil thickness (Figure 3). Our motivation for considering (7) is to enable us to explore the consequences of this form of soil production curve, with the understanding that it does not yet have a clear justification from experimental or field evidence, as does (6) [e.g., *Heimsath et al*., 1999, p. 169]. The parenthetical part of (7) may be interpreted as approximately representing the influence of increasing soil thickness on retarding water runoff, whereby the residence time of moisture and associated chemical weathering increase. Notice that as the length scale γ becomes very small, W_0 may be considered a rate of weathering of bare rock (chemical plus mechanical), and as $\kappa \to 0$, (7) reduces to (6) and W_0 retains its interpretation as in (6) (Figure 3). For later reference the maximum of (7) occurs at a soil thickness $h_1 = \gamma - 1/\kappa$. The two pairs (4) and (7) and (5) and (7) form the basis of our stability analysis presented in section 3.

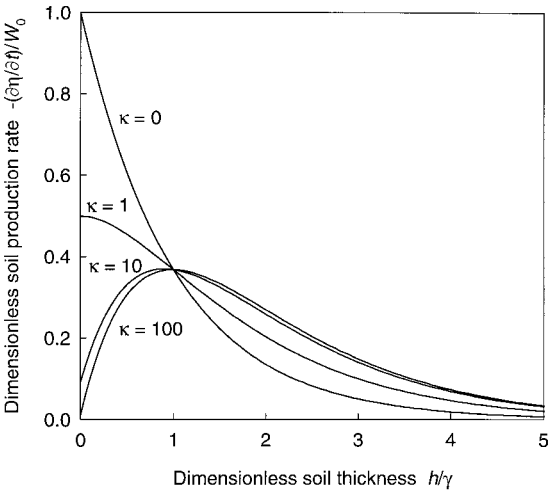

Figure 3. Diagram of dimensionless soil production rate versus dimensionless soil thickness based on equation (7) for different values of the parameter κ.

3. Linear Stability Analysis

3.1. Flux Proportional to Land Surface Gradient

Assuming for simplicity that D_V is independent of x and y and that c_h is independent of time, these quantities are removed from the differentials in (4). Then, let

$$h(x, y, t) = H + h'(x, y, t),$$
$$\eta(x, y, t) = \mathrm{H}(x, t) + \eta'(x, y, t), \tag{8}$$

where H and H are values of soil thickness and elevation, respectively, of the soil-bedrock interface associated with a basic state and h' and η' are small local fluctuations about the basic state. Substitution of (8) into (4) then provides the basic state condition:

$$\frac{\partial^2 \mathrm{H}}{\partial x^2} = \frac{c_\eta}{D_V}\frac{\partial \mathrm{H}}{\partial t}. \tag{9}$$

Substituting (8) into (7) then expanding this as an exponential series provides the additional basic state condition:

$$\frac{\partial \mathrm{H}}{\partial t} = -W_0\left(\frac{1 + \kappa H}{1 + \kappa\gamma}\right) e^{-H/\gamma} \equiv -W. \tag{10}$$

Further, substituting (10) into (9) then integrating once with respect to x gives

$$\frac{\partial \mathrm{H}}{\partial x} = -\frac{c_\eta W}{D_V} x \tag{11}$$

for $\partial \mathrm{H}/\partial x = 0$ at $x = 0$, which is equivalent to (6) of *Fernandes and Dietrich* [1997]. Together, (9), (10), and (11) characterize the steady state condition envisioned by *Gilbert* [1877, 1909], wherein the surface slope steadily increases with distance from the divide to provide the increasing soil flux necessary to accommodate steady, uniform soil production.

Using (8) through (11), (4) and (7) provide the following linearized relations involving fluctuating quantities:

$$D_V\frac{\partial^2 h'}{\partial x^2} + D_V\frac{\partial^2 h'}{\partial y^2} + D_V\frac{\partial^2 \eta'}{\partial x^2} + D_V\frac{\partial^2 \eta'}{\partial y^2} - c_h\frac{\partial h'}{\partial t} - c_\eta\frac{\partial \eta'}{\partial t} = 0, \tag{12}$$

$$W\left(\frac{1}{\gamma} - \frac{\kappa}{1 + \kappa H}\right)h' - \frac{\partial \eta'}{\partial t} = 0. \tag{13}$$

Note that a change of sign occurs in (13) when the basic state soil thickness equals that associated with the maximum soil production rate (Figure 3), namely, when $H = H_1 = \gamma - 1/\kappa$.

Relevant boundary conditions include a zero flux condition at the hillslope crest ($x = 0$) and a flux that is equal to that of the basic state at the base of the hillslope ($x = X$):

$$\left(\frac{\partial \eta'}{\partial x} + \frac{\partial h'}{\partial x}\right)_{x=0,\, x=X} = 0. \tag{14}$$

The boundary condition at $x = X$ physically coincides with a situation in which, over a period of time, the bounding stream removes sediment at a rate equal to that delivered by the basic state condition. In addition, lateral boundary conditions ($y = \pm b/2$) involve zero flux:

$$\left(\frac{\partial \eta'}{\partial y} + \frac{\partial h'}{\partial y}\right)_{y=\pm b/2} = 0. \tag{15}$$

These lateral boundaries physically represent, for example, local "divides" between swales.

It is then assumed that h' and η' can be described as doubly periodic functions:

$$h' = h_0 e^{i(m\chi x + \psi y) + \sigma t}, \qquad \eta' = \eta_0 e^{i(m\chi x + \psi y) + \sigma t}. \tag{16}$$

Here h_0 and η_0 denote complex amplitudes, σ is a complex number whose real part represents a growth rate and whose imaginary part represents a waveform celerity, i is the imaginary number defined by $i^2 = -1$, m is a waveform mode ($m = 0, 1, 2, \ldots$), and

$$\chi = \pi/X, \qquad \psi = 2\pi/b \tag{17}$$

are the fundamental wave numbers. To satisfy the boundary condition (14), the mode m sets the wave number of h' and η' to be an integer multiple of the fundamental wave number χ. Thus the first few modes ($m = 1, 2, 3, \ldots$) coincide with wavelengths of $2X$, X, $2X/3$, and so forth. (Mode $m = 0$ coincides with an infinite wavelength, which corresponds to setting h' and η' to zero.) To satisfy the boundary condition (15), the transverse wavelength is set equal to b.

Using (16), (12) and (13) become

$$-(D_V m^2\chi^2 + D_V\psi^2 + c_h\sigma)h' - (D_V m^2\chi^2 + D_V\psi^2 + c_\eta\sigma)\eta' = 0, \tag{18}$$

$$W\left(\frac{1}{\gamma} - \frac{\kappa}{1 + \kappa H}\right)h' - \sigma\eta' = 0. \tag{19}$$

Introducing the following dimensionless quantities denoted by circumflexes,

$$h' = H\hat{h}, \qquad \eta' = H\hat{\eta}, \qquad \chi = \frac{1}{X}\hat{\chi},$$
$$\psi = \frac{1}{b}\hat{\psi}, \qquad \sigma = \frac{W}{\gamma}\hat{\sigma}; \tag{20}$$

substitution into (19) leads to

$$\left(1 - \frac{\kappa\gamma}{1 + \kappa H}\right)\hat{h} - \hat{\sigma}\hat{\eta} = 0. \tag{21}$$

Using this result together with (20) and the boundary conditions (14) and (15), (18) becomes

$$\hat{\sigma}^2 + \left[\frac{\gamma}{c_h W}\left(\frac{\pi^2 m^2 D_V}{X^2} + \frac{4\pi^2 D_V}{b^2}\right) + \frac{c_\eta}{c_h}\left(1 - \frac{\kappa\gamma}{1 + \kappa H}\right)\right]\hat{\sigma} + \frac{\gamma}{c_h W}\left(1 - \frac{\kappa\gamma}{1 + \kappa H}\right)\left(\frac{\pi^2 m^2 D_V}{X^2} + \frac{4\pi^2 D_V}{b^2}\right) = 0. \tag{22}$$

According to (22) a condition of marginal stability ($\hat{\sigma} = 0$) occurs when $H = H_1 = \gamma - 1/\kappa$, that is, when the basic state soil thickness equals that associated with the maximum soil production rate (Figure 3). This result immediately allows construction of a simple stability field in terms of the dimensionless quantities H/γ and $\kappa\gamma$ (Figure 4). The line given by $(H/\gamma)_c = 1 - 1/\kappa\gamma$ separates the $H/\gamma - \kappa\gamma$ field into regions of stable and unstable behavior. For a given value of $\kappa\gamma$ an extant ratio H/γ less than the critical ratio $(H/\gamma)_c$ leads to an unstable response to a perturbation in soil thickness; this critical ratio increases with increasing $\kappa\gamma$. Moreover, because H/γ must be positive, an unstable response is possible only if $H/\gamma < 1$. For an extant ratio H/γ greater than the critical value $(H/\gamma)_c$, all remaining coefficients in (22) are positive, which requires that $\hat{\sigma} < 0$ for all $m \geq 1$ and finite values of b. This means that infinitesimal perturbations to the basic state

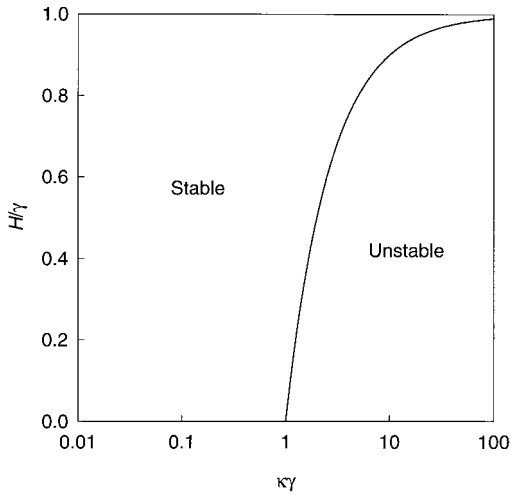

Figure 4. Stability field associated with dimensionless soil thickness H/γ versus dimensionless product $\kappa\gamma$. The line separating stable and unstable behavior is given by $(H/\gamma)_c = 1 - 1/\kappa\gamma$.

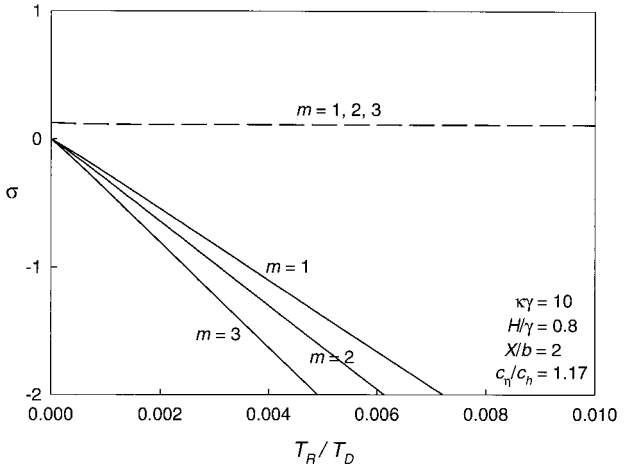

Figure 6. Plot of dimensionless growth rate $\hat{\sigma}$ versus dimensionless ratio $T_R/T_D = \gamma D_V/WX^2$ based on equation (22) showing first root (solid lines) and second root (dashed line) of $\hat{\sigma}$ for different values of mode m. The parametric values are $H = 0.4$ m, $\gamma = 0.5$ m, $X = 100$ m, $b = 50$ m, $c_\eta = 0.7$, and $c_h = 0.6$.

decay unconditionally. Note, moreover, that stability is guaranteed when $H/\gamma \geq 1$ and for the special case where $\kappa = 0$, in which (7) reduces to the exponential soil production function (6). These results are fundamentally consistent with the qualitative analysis provided by *Carson and Kirkby* [1972, p. 104–106] with reference to Figure 1.

The quantity $\hat{\sigma}$ in (22) has either two real roots or two complex conjugates. Considering the real roots first, it is useful to form the ratio T_R/T_D, where $T_R = \gamma/W$ is a measure of the mean soil particle residence time and $T_D = X^2/D_V$ is a hillslope "diffusive" timescale. For $T_R/T_D = \gamma D_V/WX^2 > 0$, one of the two real roots is everywhere negative. The other real root may be positive or negative depending on values of parametric quantities in (22), notably the product $\kappa\gamma$ (Figure 5). Together, these characterize a coupled response between the land surface and the soil-bedrock interface that involves two parts. The first is the effect of the diffusive-like behavior of soil creep which, because it tends to smooth topographic irregularities, has a universally stabilizing influence wherein perturbations in land surface elevation are damped. For $\kappa\gamma \leq 1$ both roots are negative such that the stabilizing influence on soil thickness associated with a monotonically decreasing soil production rate with increasing soil thickness reinforces the effect of land surface smoothing. For $\kappa\gamma > 1$, wherein the soil production curve possesses a part where the production rate increases with soil thickness, one of the real roots is everywhere positive over T_R/T_D. In this situation, perturbations in soil thickness or the soil-bedrock interface are amplified despite the presence of diffusive land surface smoothing.

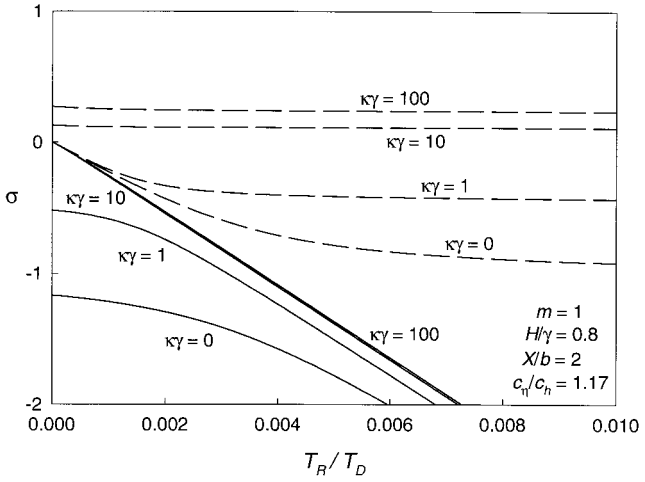

Figure 5. Plot of dimensionless growth rate $\hat{\sigma}$ versus dimensionless ratio $T_R/T_D = \gamma D_V/WX^2$ based on equation (22) showing first root (solid lines) and second root (dashed lines) of $\hat{\sigma}$ for different values of the product $\kappa\gamma$. The parametric values are $H = 0.4$ m, $\gamma = 0.5$ m, $X = 100$ m, $b = 50$ m, $c_\eta = 0.7$, and $c_h = 0.6$.

The effect of increasing mode m is to strengthen the stabilizing influence of the diffusive behavior of creep by shortening the downslope wavelength of ζ', thereby locally steepening the x component of the land surface gradient, $\partial\zeta'/\partial x$ (Figure 6). Similarly, for given hillslope length X the effect of increasing aspect ratio X/b (decreasing b) is to strengthen this stabilizing influence associated with the transverse component of creep (Figure 7). The role of the ratio c_η/c_h is to couple the rates of response of the land surface and the soil-bedrock interface. When $c_\eta/c_h = 1$, which implies an isovolumetric conversion of bedrock to soil, these responses are decoupled according to (12). One root is unconditionally negative and entirely represents (physically) diffusive land surface smoothing (Figure 8). The other root becomes constant over T_R/T_D and entirely represents the behavior of the soil-bedrock interface associated with soil production.

Turning to the complex conjugates of $\hat{\sigma}$, these exist when $F_1 < H/\gamma < F_2$, for which

$$F_1(-),\ F_2(+) = \left[1 - \frac{\pi^2 m^2 + 4\pi^2 (X/b)^2}{2c_h - c_\eta \pm 2\sqrt{c_h^2 - c_h c_\eta}} \frac{T_R}{T_D}\right]^{-1} - \frac{1}{\kappa\gamma}, \tag{23}$$

where the parenthetical sign with F_1 and F_2 designates the (middle) corresponding sign used in the denominator. Accord-

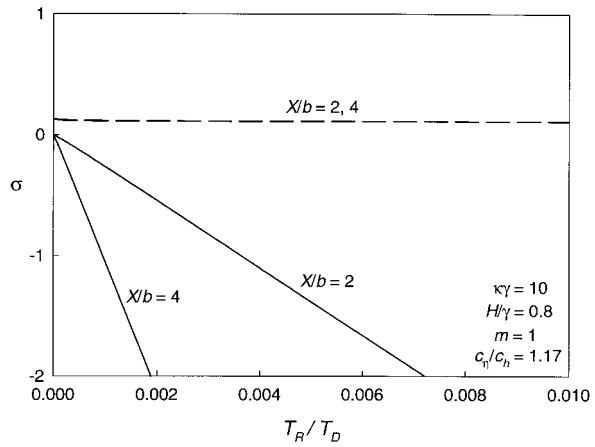

Figure 7. Plot of dimensionless growth rate $\hat{\sigma}$ versus dimensionless ratio $T_R/T_D = \gamma D_V/WX^2$ based on equation (22) showing first root (solid lines) and second root (dashed line) of $\hat{\sigma}$ for different values of the aspect ratio X/b. The parametric values are $H = 0.4$ m, $\gamma = 0.5$ m, $X = 100$ m, $c_\eta = 0.7$, and $c_h = 0.6$.

ing to (23), however, these conjugates occur only when $c_\eta < c_h$, which is physically unlikely. Thus the two roots of (22) are always real for the physically realistic case where the bedrock concentration is greater than that of the soil ($c_\eta > c_h$).

3.2. Flux Proportional to Product of Soil Thickness and Land Surface Gradient

Turning to the pair (5) and (7) and assuming that D is independent of x and y, the basic state condition (9) becomes

$$\frac{\partial^2 \mathrm{H}}{\partial x^2} = \frac{c_\eta}{DH}\frac{\partial \mathrm{H}}{\partial t}, \tag{24}$$

and (11) becomes

$$\frac{\partial \mathrm{H}}{\partial x} = -\frac{c_\eta W}{DH}x. \tag{25}$$

The linearized relation involving fluctuating quantities is

$$DH\frac{\partial^2 h'}{\partial x^2} + DH\frac{\partial^2 h'}{\partial y^2} - \frac{c_\eta W}{H}x\frac{\partial h'}{\partial x} - \frac{c_\eta W}{H}h' + DH\frac{\partial^2 \eta'}{\partial x^2} + DH\frac{\partial^2 \eta'}{\partial y^2} - c_h\frac{\partial h'}{\partial t} - c_\eta\frac{\partial \eta'}{\partial t} = 0 \tag{26}$$

Notice that the third term in (26) has a coefficient that depends on x. Boundary conditions analogous to (14) are

$$\left(\frac{\partial \eta'}{\partial x} + \frac{\partial h'}{\partial x}\right)_{x=0} = 0, \qquad \left(\frac{\partial \eta'}{\partial x} + \frac{\partial h'}{\partial x} - \frac{c_\eta WX}{DH^2}h'\right)_{x=X} = 0. \tag{27}$$

It is then assumed that

$$h' = h_0 f(x)e^{i\psi y + \sigma t}, \qquad \eta' = \eta_0 f(x)e^{i\psi y + \sigma t}. \tag{28}$$

In this formulation, $f(x)$ does not necessarily contain a parametric quantity describing a length scale over which h' and η' vary, analogous to χ in (16). Making use of the dimensionless quantities in (20) and (21),

$$\frac{\partial^2 \hat{h}}{\partial \hat{x}^2} + \frac{X^2}{b^2}\frac{\partial^2 \hat{h}}{\partial \hat{y}^2} - \frac{c_\eta WX^2\hat{\sigma}}{DH^2\left[\left(1 - \dfrac{\kappa\gamma}{1+\kappa H}\right) + \hat{\sigma}\right]}\hat{x}\frac{\partial \hat{h}}{\partial \hat{x}} - \frac{WX^2}{DH\left[\left(1 - \dfrac{\kappa\gamma}{1+\kappa H}\right) + \hat{\sigma}\right]} \cdot \left\{c_\eta\left[\frac{1}{H} + \frac{1}{\gamma}\left(1 - \frac{\kappa\gamma}{1+\kappa H}\right)\right]\hat{\sigma} + \frac{c_h}{\gamma}\hat{\sigma}^2\right\}\hat{h} = 0, \tag{29}$$

where the boundary conditions in (27) become

$$\left(\frac{\partial \hat{h}}{\partial \hat{x}}\right)_{\hat{x}=0} = 0, \qquad \left\{\frac{\partial \hat{h}}{\partial \hat{x}} - \frac{c_\eta WX^2}{\left[\left(1 - \dfrac{\kappa\gamma}{1+\kappa H}\right) + \hat{\sigma}\right]DH^2}\hat{h}\right\}_{\hat{x}=1} = 0. \tag{30}$$

Solutions of (29) and (30) consist of confluent hypergeometric functions [*Abramowitz and Stegun*, 1965, p. 503–535] which generally must be evaluated numerically. Relevant examples are presented below. Meanwhile, we examine one important analytical solution that exists.

To simplify the coefficient notation, (29) is rewritten as

$$\frac{\partial^2 \hat{h}}{\partial \hat{x}^2} + A\frac{\partial^2 \hat{h}}{\partial \hat{y}^2} - B\hat{x}\frac{\partial \hat{h}}{\partial \hat{x}} - C\hat{h} = 0. \tag{31}$$

Here we assume a solution of the form

$$\hat{h} = \hat{h}_0 \exp(E\hat{x}^2 + i\hat{\psi}\hat{y}), \tag{32}$$

where $\hat{h}_0$ denotes the value of $\hat{h}$ at $\hat{x} = 0$. This leads to

$$2E(2E - B)\hat{x}^2 + 2E - A\hat{\psi}^2 - C = 0, \tag{33}$$

which is satisfied when $B = 2E$ and $C = B - A\hat{\psi}^2$ or when

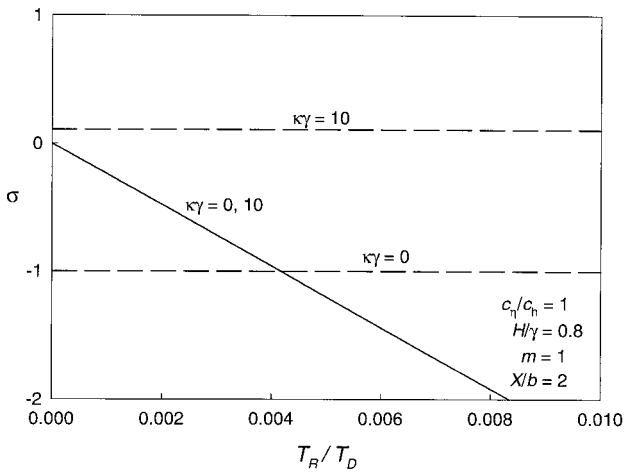

Figure 8. Plot of dimensionless growth rate $\hat{\sigma}$ versus dimensionless ratio $T_R/T_D = \gamma D_V/WX^2$ based on equation (22) showing first root (solid line) and second root (dashed lines) of $\hat{\sigma}$ for different values of the product $\kappa\gamma$ and the special case of $c_\eta/c_h = 1$. The parametric values are $H = 0.4$ m, $\gamma = 0.5$ m, $X = 100$ m, $b = 50$ m, $c_\eta = 0.7$, and $c_h = 0.7$.

$$\hat{\sigma}^2 + \left[\frac{c_\eta}{c_h}\left(1 - \frac{\kappa\gamma}{1 + \kappa H}\right) + \frac{4\pi\gamma DH}{c_h WX^2}\frac{X^2}{b^2}\right]\hat{\sigma} + \frac{4\pi\gamma DH}{c_h WX^2}\frac{X^2}{b^2}\left(1 - \frac{\kappa\gamma}{1 + \kappa H}\right) = 0. \quad (34)$$

In turn, $E = B/2$, so the solution (32) looks like

$$\hat{h} = \hat{h}_0 \exp\left\{\frac{c_\eta WX^2\hat{\sigma}}{2DH^2\left[\left(1 - \frac{\kappa\gamma}{1 + \kappa H}\right) + \hat{\sigma}\right]}\hat{x}^2 + i\hat{\psi}\hat{y}\right\}, \quad (35)$$

which is monotonic in $\hat{x}$ and periodic in $\hat{y}$.

According to (34) a condition of marginal stability ($\hat{\sigma} = 0$) occurs when $H = H_1 = \gamma - 1/\kappa$, and it follows that the simple stability field involving H/γ and $\kappa\gamma$, as described in the preceding analysis (Figure 4), also applies to this case. Moreover, the quantity $\hat{\sigma}$ in (34) has two real roots whose interpretation, and behavior, is similar to that of the two roots of (22) described above (Figure 9).

Additional solutions of (29) and (30) can be evaluated numerically with integration of (29) using a shooting technique [*Press et al.*, 1986, p. 578–588]. These solutions consist of a set of oscillating curves whose amplitudes increase downslope (Figure 10) and whose (integer) number of zero crossings is analogous to the mode m in the previous analysis involving sinusoidal solutions of η' and ζ'. The behavior of the two roots of $\hat{\sigma}$ is similar to that associated with the monotonic solution (35) presented above. The effect of increasing number of zero crossings is like that of increasing mode m in the previous analysis, to strengthen the stabilizing influence of diffusive land surface smoothing with respect to the downslope direction.

4. Implications for Hillslope Evolution

4.1. Time-Varying Boundary Conditions

The preceding analysis assumes, for convenience, a steady, uniform rate W of land surface lowering, which implies steady downcutting by a stream at the lower hillslope boundary at the same rate W (measured relative to the uplift rate). It is arguable, however, whether this condition occurs for any significant period in nature, and so it is important to consider the influence of time variations in the lower boundary condition [e.g., *Armstrong*, 1987] (also see review by *Fernandez and Dietrich* [1997, p. 1307–1308]).

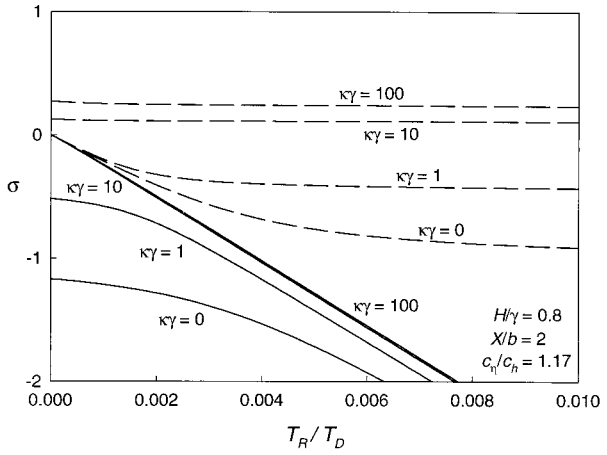

Figure 9. Plot of dimensionless growth rate $\hat{\sigma}$ versus dimensionless ratio $T_R/T_D = \gamma DH/WX^2$ based on equation (34) showing first root (solid lines) and second root (dashed lines) of $\hat{\sigma}$ for different values of the product $\kappa\gamma$. The parametric values are $H = 0.4$ m, $\gamma = 0.5$ m, $X = 100$ m, $b = 50$ m, $c_\eta = 0.7$, and $c_h = 0.6$; compare with Figure 5.

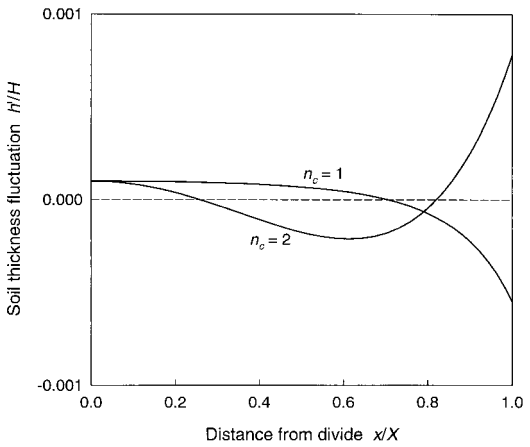

Figure 10. Plot of numerical solutions to equations (29) and (30) for number of zero crossings $n_c = 1, 2$. The parametric values are $c_\eta = 0.7$, $c_h = 0.6$, $X/b = 4$, $T_R/T_D = \gamma DH/WX^2 = 0.1$, and $\hat{h} = 0.0001$.

Whereas a stream may be capable of lowering its bedrock surface [e.g., *Sklar and Dietrich*, 1998], a change in the rate of lowering of the soil-bedrock interface at a finite distance from the stream, relative to the rate of lowering of the basic state, must involve the coupling between the soil production rate and soil thickness. This means that a local change in the soil-bedrock interface (about the basic state) must be initiated by a local change in soil thickness (and therefore land surface elevation). Thus, to describe changes in the lower boundary condition, we specify changes in the land surface elevation at this position and allow the soil-bedrock interface to respond accordingly.

Here it is momentarily convenient to adopt a coordinate system whose horizontal axis is positive in the upslope direction with origin at the lower boundary. Letting s denote this axis, we apply the transformation $s = X - x$. It is also convenient to describe the land surface elevation $\zeta(0, t)$ as a periodic function:

$$\zeta(0, t) = Z(0, t) + \zeta'(0, t) = Z(0, t) + A_\zeta \cos(\omega t), \quad (36)$$

where Z is the basic state elevation, A_ζ is the amplitude of fluctuations in $\zeta'(0, t)$, and $\omega = 2\pi/T$ is the angular frequency with period T. In turn, the rate of lowering at $s = 0$ is

$$\frac{\partial\zeta(0, t)}{\partial t} = -W + \frac{\partial\zeta'(0, t)}{\partial t} = -W - A_\zeta\omega \sin(\omega t), \quad (37)$$

where we insist that $|A_\zeta\omega| \leq |W|$, ensuring that neither $\zeta(s, t)$ nor $\eta(s, t)$ increases in an absolute sense (which would imply an increase in land surface elevation due to net deposition and a "reversal" of bedrock-to-soil conversion, respectively). Note that when $A_\zeta\omega - W = 0$, the elevation $\zeta(0, t)$ is unchanging in a global reference frame. Thus (37) describes a periodic waxing and waning of stream downcutting about a mean lowering rate W.

For the case where the soil flux is proportional to the land surface gradient, as in (2), and when $\kappa = 0$ in (7), the coupled

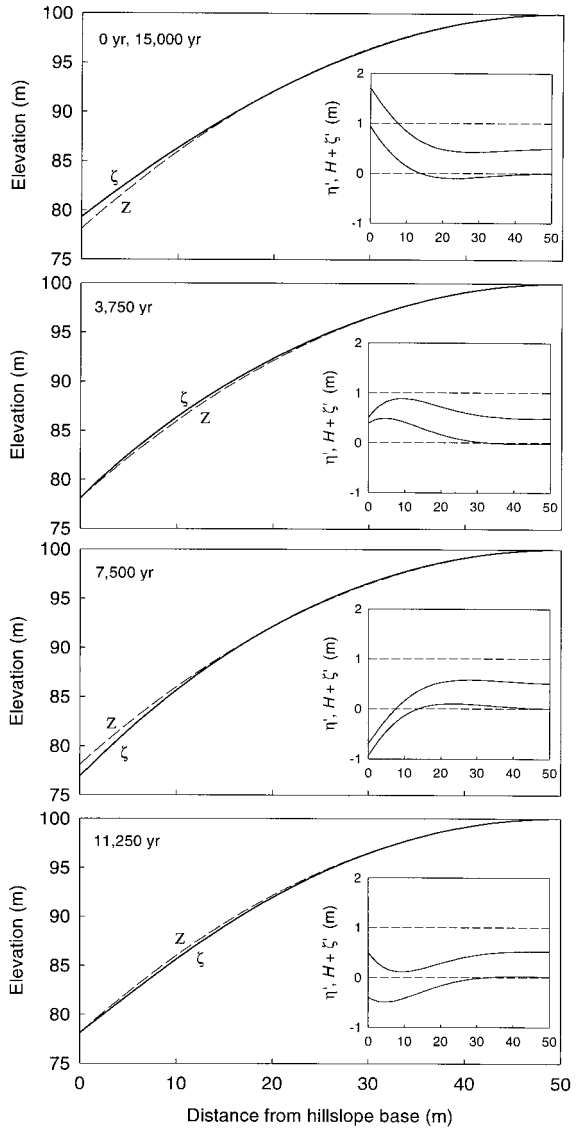

Figure 11. Plot of hillslope land surface ζ (solid lines) responding to sinusoidal variation (T = 15,000 years) in downcutting rate at lower boundary, relative to steadily lowering basic state Z (dashed lines), with corresponding fluctuations in soil-bedrock interface η' and land surface ζ' about basic states H and $Z = H + H$ (insets). The parametric values are H = 0.5 m, $c_\eta = 0.7$, $c_h = 0.6$, $\gamma = 0.5$ m, $D_V = 0.02$ m^2 yr^{-1}, and $W = 0.0005$ m yr^{-1}.

equations (4) and (7) are nonlinear only because (7) involves the exponential function (assuming constant c_h). This nonlinearity, moreover, is very weak for small perturbations η', h', and ζ'. For this reason (and simplicity) we examine the response of a soil-mantled hillslope to the boundary condition (36) using the linear forms (12) and (13) with $\kappa = 0$ (Appendix A). In this situation we also apply the more restrictive constraint that $|A_\zeta \omega| < |W_0|$, ensuring that $\zeta(s, t)$ is not lowered to the level of $\eta(s, t)$, which would imply exposure of bedrock.

Specifically, $\zeta(s, t)$ and $\eta(s, t)$ are given by

$$\zeta(s, t) = \mathrm{Z}(s, t) + A_\zeta \cos(ks - \omega t)e^{-ks}, \quad (38)$$

$$\eta(s, t) = \mathrm{H}(s, t) + A_\zeta G \cos(ks - \omega t + \phi)e^{-ks}, \quad (39)$$

where, in our redefined coordinate system with the hillslope crest at $s = X$,

$$\mathrm{H}(s, t) = -\frac{c_\eta W}{2D_V}(X - s)^2 + \mathrm{H}(X, t), \quad \mathrm{Z}(s, t) = \mathrm{H}(s, t) + H. \quad (40)$$

Further, k and ϕ in (38) and (39), respectively, denote a wave number and a phase shift given by

$$k = \left\{\frac{c_h[G(c_\eta/c_h - 1) + 1]\omega}{2D_V}\right\}^{1/2}, \qquad \phi = \tan^{-1}\left(\frac{\gamma\omega}{W}\right) = \tan^{-1}\left(\frac{2\pi T_R}{T}\right), \quad (41)$$

and G is a gain (the ratio of the amplitudes of η' and ζ') given by

$$G = [1 + (\gamma\omega/W)^2]^{-1} = \lfloor 1 + (2\pi T_R/T)^2 \rfloor^{-1}. \quad (42)$$

Together, (38) and (39) describe a coupled response, between the land surface $\zeta(s, t)$ and the soil-bedrock interface $\eta(s, t)$, to the periodic boundary condition defined by (36) and (37). Specifically, a change in ζ involves a change in h, which leads to a change in η via the soil production function (6); this change in η, in turn, leads to a response in ζ via nonisovolumetric conversion of bedrock to soil, characterized by the factor $(c_\eta/c_h - 1)$ in (41). Note that when $c_\eta/c_h - 1$ (an isovolumetric conversion), this latter feedback vanishes according to (A1). That is, conversion of a unit of bedrock produces a unit increase in soil thickness without a change in land surface elevation; then $\zeta(s, t)$ becomes a simple forcing function, and $\eta(s, t)$ is the response according to (A2).

This coupled response has the form of damped waveforms that propagate upslope, where the land surface waveform leads the soil-bedrock interface waveform (Figure 11). The trough of $\zeta'(s, t)$ is a site of relatively high soil production, so $\eta'(s, t)$ is lowered as this trough passes over. The depression in $\eta'(s, t)$ then persists as the production rate declines with thickening soil behind the trough. Then, the rate of lowering W of the mean state exceeds the rate of lowering of the soil-bedrock interface such that $\eta'(s, t)$ eventually becomes positive until the next trough of $\zeta'(s, t)$ passes over. Thus it is important to recognize that in plots involving $\zeta'(s, t)$ and $\eta'(s, t)$, a state where $\eta'(s, t) > 0$ does not represent an increase in elevation of this interface in an absolute reference frame (a "reversal" of bedrock-to-soil conversion); rather, this marks a state where the mean rate of lowering W momentarily exceeds the rate of lowering of $\eta(s, t)$.

For given soil-mantle properties the gain G increases, and the phase ϕ decreases, with the ratio of the period T to the mean soil particle residence time T_R. With large T/T_R, the land surface elevation changes sufficiently slowly that the rate of soil production hovers close to the mean rate W, thereby maintaining a nearly uniform soil thickness ($G \to 1$ and $\phi \to 0$). With small T/T_R, soil production lags, manifest as an increasing phase and decreasing amplitude of the response in $\eta'(s, t)$. In effect, $\eta(s, t)$ is insensitive to short-term variations in downcutting rate and responds nearly synchronously with the land surface with long-term variations.

A measure of the distance λ_w of waveform propagation is $\lambda_w = 1/k$, which, for typical soil conditions and rates of land surface lowering, is well approximated by $\lambda_w \approx \sqrt{D_V/\omega}$. Thus even for large values of D_V, $O[0.01$ m^2 yr$^{-1}]$, λ_w is only a few

tens of meters over a period $T = 100{,}000$ years. This suggests that the upper part of a long hillslope may be relatively insensitive to short-term variations in downcutting rate at the lower boundary. Specifically, the ratio

$$\frac{\lambda_w}{X} \approx \sqrt{\frac{D_V T}{2\pi X^2}} \sim \sqrt{\frac{T}{T_D}} \tag{43}$$

indicates that the uppermost part of a hillslope "feels" the lower boundary only when the period T approaches (or exceeds) the "diffusive" timescale T_D.

The magnitude of the soil flux to the stream per unit contour distance $Q(0, t) = hq_s(0, t) = D_V \partial\zeta/\partial s|_{s=0}$, or

$$Q(0, t) = c_\eta WX - D_V A_\zeta k[\cos(\omega t) - \sin(\omega t)]. \tag{44}$$

The first term on the right side of (44) is the steady basic state contribution; the second term on the right is a fluctuation about the basic state flux. The maximum soil flux thus occurs $T/8$ before ζ' reaches its minimum (negative) value or $T/8$ after the maximum rate of downcutting.

The response to similar, periodic lower-boundary conditions involving a flux that is proportional to the product of soil thickness and land surface gradient, as in (3), requires a numerical solution. Toward this end, initial numerical experiments suggest that the nonlinearity introduced by (3) leads to behavior wherein the magnitude and timing of sediment delivery to a stream does not map as a simple response to downcutting rate. Rather, delivery responds in a complex, sensitive manner to the initial state of the soil and hillslope morphology and to the period and amplitude of downcutting. With sufficient soil thickness H for specified γ and D, delivery is nearly in phase with the downcutting rate, similar to the linear formulation above. Near the boundary the soil thins as the land surface steepens with accelerated downcutting. The effect of steepening dominates over decreasing soil thickness, so the net effect is increasing transport. With smaller H for the same γ and D the effect of soil thinning dominates over steepening, so transport is nearly out of phase with the downcutting rate, counter to the linear case. In addition, the amplitude of the delivery rate is much smaller than for the linear case. In addition, internal adjustments between slope, soil thickness, and soil production rate produce complex transport rate signals away from the boundary, and this response is much more strongly attenuated with upslope distance than is the linear response.

There is also the likelihood that certain parametric values vary over the periods considered here, for example, the diffusion-like coefficient D_V [e.g., *Fernandes and Dietrich*, 1997] and the length scale of soil production γ [e.g., *Heimsath et al*., 1999, p. 167]. Whereas we have for simplicity set these as constants in the preceding analysis, effects of varying D_V (or D) and γ deserve further examination. Here again, initial numerical experiments suggest that time variations in these parametric quantities may significantly complicate hillslope response to downcutting as measured, say, by the delivery rate $Q(0, t)$. However, to fully clarify these effects will require a better understanding of how these parametric quantities are related to each other and possibly covary with downcutting rate.

4.2. Spatial Variations in Soil Production Rate

The basic state considered in the preceding stability analysis involves a uniform soil mantle of thickness H covering a convex (parabolic) bedrock surface $\mathrm{H}(x, t)$. This basic state provides an unambiguous reference point for the linear stability analysis

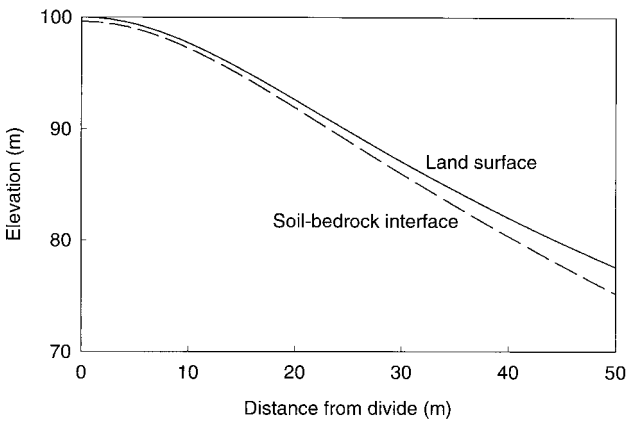

Figure 12. Plot of land surface and soil-bedrock interface of convex-concave hillslope undergoing steady, uniform lowering for the case where soil production length scale γ increases downslope according to $\gamma = \gamma_0 + \beta x^n$. *The parametric values are* $W = 0.0002$ m yr^{-1}, $D = 0.01$ m yr^{-1}, $H_0 = 0.4$ m, $\gamma_0 = 0.5$ m, $\beta = 0.001$ m^{1-n}, and $n = 2$.

and has the additional appeal that it represents the condition of uniform land surface lowering originally envisioned by *Gilbert* [1877, 1909]. It is, nonetheless, important to emphasize that other basic states involving steady, uniform lowering are possible. Consider, for example, the possibility that the rate of soil production, for given soil thickness, increases with downslope distance. On heuristic grounds one can envision that increasing soil water circulation and residence time in a downslope direction lead to a concomitant increase in chemical weathering that is reflected in the soil production length scale. For example, assuming a locally monotonic relation with soil thickness h,

$$\frac{\partial \eta}{\partial t} = -W_0 e^{-h/(\gamma_0 + \beta x^n)}, \tag{45}$$

where γ_0 is the soil production length scale at the divide ($x = 0$), β [L^{1-n}] is a rate of increase in this length scale with downslope distance x, and n is an exponent.

Considering the basic state quantities $\mathrm{H}(x, t)$, $H(x)$, and $\mathrm{Z}(x, t) = \mathrm{H}(x, t) + H(x)$, the rate of soil production at the divide is $\partial \mathrm{H}_0/\partial t = -W_0 \exp(-H_0/\gamma_0)$. With uniform lowering rate W this implies that $-W \equiv -W_0 \exp(-H_0/\gamma_0) = -W_0 \exp[-H/(\gamma_0 + \beta x^n)]$ or

$$H(x) = H_0\left(1 + \frac{\beta}{\gamma_0} x^n\right). \tag{46}$$

In turn,

$$\frac{\partial \mathrm{Z}}{\partial x} = -\frac{c_\eta W}{DH_0} \frac{x}{1 + (\beta/\gamma_0)x^n}. \tag{47}$$

Taking the derivative of (47) with respect to x and setting the result to zero then leads to

$$x_1 = \left[\frac{\gamma_0}{\beta(n-1)}\right]^{1/n}. \tag{48}$$

This indicates that, for $\beta > 0$ and $n > 1$, the profile $\mathrm{Z}(x)$ generally possesses an inflection at $x = x_1 > 0$. That is, $\mathrm{Z}(x)$ describes a convex-concave land surface, assuming that $x_1 < X$ (Figure 12). (Also note that specific cases of $n < 1$, for example, the series $n = 1/2, 1/4, 1/6, \ldots$, provide permis-

sible solutions of (48).) This is in contrast to conventional thinking that a steady, uniform erosional state involving a diffusive-like process leads to a convex hillslope form.

5. Discussion and Conclusions

The model described in section 2 fully couples the behavior of land surface geometry, soil transport, soil thickness, and soil production for the case of soil-mantled hillslopes undergoing diffusive creep. This provides the important possibility of numerically simulating the coevolution of the land surface and soil thickness of a complex landscape, including real landscapes for which land surface elevation and soil data are available at sufficient resolution [e.g., *Heimsath et al*., 1999]. Equally important, the formal framework of the stability analysis presented herein provides a concise, complementary way of characterizing key aspects of this coupled behavior, notably consequences of the soil production relation (Figures 1 and 3), that may bear more generally on interpreting diffusive landscapes.

The fully coupled behavior of land surface geometry, soil transport, soil thickness, and soil production strongly hinges on the form of the relation between the soil production rate and soil thickness. The detailed form of the relation (7) between the soil production rate and soil thickness is heuristic, with clear field justification present only for the monotonically decreasing part of it. With this caveat the stability analysis suggests that the response to a perturbation in soil thickness is fundamentally consistent with the qualitative analysis provided by *Carson and Kirkby* [1972, p. 104–106], that perturbations are damped for extant (initial) soil conditions to the right of the maximum in Figure 1 and are unstably amplified for conditions to the left of the maximum. This behavior involves two parts. The first is associated with the land surface, wherein perturbations are unconditionally damped because of the diffusive smoothing of soil creep. The second part involves a response to disturbances in soil thickness or the soil-bedrock interface via the dependence of soil production rate on soil thickness and may be stable or unstable. These two parts generally are coupled via nonisovolumetric conversion of bedrock to soil ($c_\eta/c_h \neq 1$) but become decoupled with isovolumetric conversion ($c_\eta/c_h = 1$). The analysis also suggests that this behavior is insensitive to the transport relation involved, whether the volumetric flux $h\mathbf{q}$ is proportional to the land surface gradient, as in (2), or to the product of the soil thickness and land surface gradient, as in (3) (compare Figures 5 and 9). This point is important because it means that the nonlinearity introduced by (3) does not fundamentally change the hillslope response to small disturbances from that associated with a purely linear transport relation.

It is important to note that our stability analysis formally pertains to small perturbations in the elevation of the land surface or soil-bedrock interface about a basic state that involves steady, uniform lowering; it does not characterize finite amplitude behavior. This is likely of less significance for conditions involving a stable behavior (where both roots of $\hat{\sigma}$ in either (22) or (29) are negative) than for conditions where disturbances in soil thickness are amplified. In this latter case a complete description of how the soil mantle responds to disturbances requires solving the basic (nonlinearized) equations. The analysis, moreover, assumes that the active transport thickness coincides with the soil thickness, as measured from the land surface to the soil-bedrock interface. This is certainly reasonable for net erosive hillslopes where the position of the soil-bedrock interface is largely set by biomechanical activity which simultaneously contributes to diffusive soil transport as characterized by (2) or (3). It may be less justified for deeply weathered soil regolith conditions if the zone of active transport is well above the lowermost soil boundary as defined pedologically.

Whereas the stability analysis reveals important details regarding the general response of a soil-mantled hillslope to disturbances in soil thickness, the significance of this behavior becomes clearer in the context of a hillslope that is affected by conditions at its boundaries, notably its lower boundary where stream downcutting rates vary, and influence hillslope behavior on geomorphic timescales. Specifically, a periodic (sinusoidal) variation in downcutting leads to a coupled response between the land surface and soil-bedrock interface that has the form of damped waveforms propagating upslope (Figure 11). The land surface waveform leads the soil-bedrock waveform, where the gain and phase between them are strongly influenced by the period T of downcutting. Of particular significance is that the distance of waveform propagation increases approximately as the square root of the product of the period T and the diffusion-like coefficient D_V. This generally means that the behavior of the upper part of the hillslope is insensitive to short-term variations in downcutting rate and "feels" the effect of the lower boundary only when the period T approaches the diffusive (relaxation) timescale of the hillslope ($T_D = X^2/D_V$), that is, with $D_V = O[10^{-2}\ \mathrm{m^2\ yr^{-1}}]$, when $T \sim 10^6$ years for $X = O[10^2\ \mathrm{m}]$ or when $T \sim 10^4$ years for $X = O[10\ \mathrm{m}]$. These points are entirely consistent with conclusions of *Fernandes and Dietrich* [1997] derived from numerical experiments involving responses to step changes in downcutting rate, that response times increase with hillslope length X and decrease with the diffusion-like coefficient D_V and that relative upslope propagation of the effects of the imposed boundary condition diminishes with this response time (7×10^4 years and 1×10^6 years for $X = 25$ m and $X = 100$ m, respectively).

By comparison, the modeling work of *Dietrich et al*. [1995] and *Heimsath et al*. [1999] suggests that locally the soil thickness on the upper parts of creep-dominated hillslopes can approach a steady state condition over a period of less than 10,000 years. Thus, if a hillslope approaches (or reaches) a stable morphology with respect to diffusive erosion, soil thickness, and soil production and if the prevailing relation between the soil production rate and soil thickness is such that the response of the soil mantle to disturbances is a stable one, then in the absence of long-term variations in stream downcutting the upper part of such a hillslope may exhibit an approximately steady behavior as envisioned by *Gilbert* [1877, 1909], while the lower part responds transiently to the lower boundary conditions. One might therefore expect to find relatively uniform topographic curvature and soil thickness near the upper parts of hillslopes, with increasing variability in curvature and thickness downslope reflecting unsteady conditions associated with a complex history of stream downcutting [e.g., *Heimsath et al*., 1999]. Conversely, in the presence of long-term variations in stream downcutting, and depending on the initial state, hillslope morphology and soil thickness variations are more likely to reflect unsteady conditions over the entirety of the hillslope [*Fernandes and Dietrich*, 1997]. The possibility also exists that, if the prevailing relation between the soil production rate and soil thickness is such that the soil mantle responds unstably to disturbances, the response of a hillslope to variations in downcutting rate might force the soil mantle across a critical soil

thickness state (Figure 4), leading to an unstable behavior (and possibly complex distribution of soil thickness), although field-based evidence for the existence of this type of soil production relation remains to be demonstrated.

Several caveats deserve comment. Our analysis of effects of variations in the downcutting rate at the lower boundary neglects the possibility of time variations in the values of parametric quantities, notably the diffusion-like coefficient D_V and the length scale of soil production γ, which are likely to change over geomorphically significant periods [*Fernandes and Dietrich*, 1997; *Heimsath et al*., 1999]. To fully clarify the effects of such variations will require understanding how these parametric quantities covary with downcutting rate which, in turn, will require further understanding of how, for example, climatic variations influence both. The analysis also treats the hillslope away from the lower boundary as an infinite half-space with boundary conditions $\zeta'(\infty, t) = 0$ and $\eta'(\infty, t) = 0$. These conditions are strictly applicable only when the ratio of the upslope distance of waveform propagation to the hillslope length $\lambda_w/X \ll 1$, which means that the periodic solutions given by (38) and (39) do not necessarily satisfy a zero-flux condition at the hillslope divide when $\lambda_w/X \to 1$. In addition, the analysis neglects transient "start-up" effects in the periodic solutions given by (38) and (39). Although these omissions do not detract from the essential conclusions of the analysis, they, nonetheless, highlight that other possible boundary conditions may be relevant in a full description of hillslope response [*Armstrong*, 1987]. For example, the boundary condition (36) specifies the land surface position at the stream, such that the soil flux at this position, given by (44), is an outcome. One may alternatively specify this boundary condition in terms of the soil flux as determined by the behavior of the stream, its propensity to remove sediment from the base of the hillslope, such that the land surface and soil-bedrock interface respond to this behavior.

Convex-concave hillslope forms may arise from combinations of a variety of initial states, transport processes, and boundary conditions, involving both steady and unsteady behavior. Because soil production is a fundamental part of this behavior, possible effects of spatial variations in soil production rate should be added to this set of factors affecting hillslope forms. To illustrate this point, we present the heuristic example where the production rate, for given soil thickness, increases with downslope position for hydrogeochemical reasons. For transport that is proportional to the product of soil thickness and land surface gradient, as in (3), this variation in production rate leads to a convex-concave form with increasing soil thickness downslope under the simplest possible conditions of steady, uniform lowering (Figure 12), a situation that is not normally attributed to purely diffusive transport. (The existence of such a state could be readily tested; a first requirement would be to demonstrate uniform soil production with position and soil thickness (A. Heimsath, personal communication, 1999) based on, say, cosmogenic isotope measurements.) This reinforces the idea that a convex-concave form is not necessarily diagnostic of a particular transport process or state of hillslope evolution (nor does it necessarily imply steady, uniform lowering with varying production rate). It also suggests that the idea that transport is proportional to the product of soil thickness and land surface gradient [*Ahnert*, 1967; *Furbish and Dietrich*, 1999, 2000; *Braun et al*., 2000] deserves further examination, as the existence of such a transport relation could lead to more complex hillslope forms than might otherwise be expected for diffusive transport.

Appendix A

For the one-dimensional case with $s = X - x$ and $\kappa = 0$ we rewrite (12) and (13) as

$$\frac{D_V}{c_h}\frac{\partial^2 \zeta'}{\partial s^2} - \frac{\partial \zeta'}{\partial t} - \left(\frac{c_\eta}{c_h} - 1\right)\frac{\partial \eta'}{\partial t} = 0 \tag{A1}$$

$$\frac{W}{\gamma}\,\zeta' - \frac{W}{\gamma}\,\eta' - \frac{\partial \eta'}{\partial t} = 0 \tag{A2}$$

respectively, then assume solutions of the form

$$\zeta'(s, t) = A_\zeta e^{i(ks-\omega t)} e^{-ks} \tag{A3}$$

$$\eta'(s, t) = A_\eta e^{i(ks-\omega t)} e^{-ks}, \tag{A4}$$

where A_ζ is a real amplitude and A_η is complex.

Substituting (A3), (A4), and the first derivative of (A4) with respect to time t into (A2) leads to

$$\frac{A_\eta}{A_\zeta} = \left(1 - i\,\frac{\gamma\omega}{W}\right)^{-1}. \tag{A5}$$

The gain G is obtained as the modulus of the right side of (A5), which is given by (42) in the text. The phase ϕ is obtained as the angle of the right side of (A5), or $\phi = -\tan^{-1}(-\gamma\omega/W) = \tan^{-1}(\gamma\omega/W)$, which is the second part of (41) in the text.

Substituting the second derivative of (A3) with respect to position s and the first derivatives of (A3) and (A4) with respect to time t into (A1) leads to

$$-\frac{2D_V}{c_h}k^2 + \omega + \left(\frac{c_\eta}{c_h} - 1\right)G\omega = 0. \tag{A6}$$

Solving for the wave number k then gives the first part of (41) in the text.

Acknowledgments. We are grateful to David Loper and Ruby Krishnamurti for providing thoughtful insight regarding the stability analysis and to Peter Haff and Arjun Heimsath for their continued input and review of our work.

References

Abramowitz, M., and I. A. Stegun, *Handbook of Mathematical Functions*, Dover, Mineola, N. Y., 1965.

Ahnert, F., The role of the equilibrium concept in the interpretation of landforms of fluvial erosion and deposition, in *L'evolution des Versants*, edited by P. Macar, pp. 23–41, Univ. of Liege, Liege, France, 1967.

Armstrong, A. C., Slopes, boundary conditions, and the development of convexo-concave forms—Some numerical experiments, *Earth Surf. Processes Landforms*, *12*, 17–30, 1987.

Braun, J., A. M. Heimsath, and J. Chappell, On the nature of sediment transport mechanisms on hillslopes, *Eos Trans. AGU*, *81*(47), Fall Meet. Suppl., abstract H-12B-12, 2000.

Bucknam, R. C., and R. E. Anderson, Estimation of fault-scarp ages from a scarp-height-slope-angle relation, *Geology*, *7*, 11–14, 1979.

Carson, M. A., and M. J. Kirkby, *Hillslope Form and Process*, Cambridge Univ. Press, New York, 1972.

Culling, W. E. H., Soil creep and the development of hillside slopes, *J. Geol*., *71*, 127–161, 1963.

Culling, W. E. H., Theory of erosion on soil-covered slopes, *J. Geol*., *73*, 230–254, 1965.

Dietrich, W. E., R. Reiss, M. Hsu, and D. R. Montgomery, A process-

based model for colluvial soil depth and shallow landsliding using digital elevation data, *Hydrol. Processes*, *9*, 383–400, 1995.

Fernandes, N. F., and W. E. Dietrich, Hillslope evolution by diffusive processes: The timescale for equilibrium adjustments, *Water Resour. Res*., *33*, 1307–1318, 1997.

Furbish, D. J., and W. E. Dietrich, On the use of a diffusion-like equation to describe hillslope evolution by soil creep (abstract), *Eos. Trans. AGU*, Fall Meet. Suppl., *80*(46), F444–F445, 1999.

Furbish, D. J., and W. E. Dietrich, The diffusion-like coefficient in hillslope evolution models described in terms of the frequency and magnitude of soil particle motions associated with biological activity (abstract), *Geol. Soc. Am. Abstr. Programs*, *32*(7), A-117, 2000.

Gilbert, G. K., Geology of the Henry Mountains (Utah), report, U.S. Geogr. and Geol. Surv. of the Rocky Mt. Reg., Washington, D. C., 1877.

Gilbert, G. K., The convexity of hilltops, *J. Geol*., *17*, 344–350, 1909.

Heimsath, A. M., W. E. Dietrich, K. Nishiizumi, and R. C. Finkel, The soil production function and landscape equilibrium, *Nature*, *388*, 358–361, 1997.

Heimsath, A. M., W. E. Dietrich, K. Nishiizumi, and R. C. Finkel, Cosmogenic nuclides, topography, and the spatial variation of soil depth, *Geomorphology*, *27*, 151–172, 1999.

Hirano, M., Simulation of developmental process of interfluvial slopes with reference to graded form, *J. Geol*., *83*, 113–123, 1975.

Jyotsna, R., and P. K. Haff, Microtopography as an indicator of modern hillslope diffusivity in arid terrain, *Geology*, *25*, 695–698, 1997.

Kirkby, M. J., Measurement and theory of soil creep, *J. Geol*., *75*, 359–378, 1967.

McKean, J. A., W. E. Dietrich, R. C. Finkel, J. R. Southon, and M. W. Caffee, Quantification of soil production and downslope creep rates from cosmogenic ^{10}Be accumulations on a hillslope profile, *Geology*, *21*, 343–346, 1993.

Nash, D., Forms of bluffs degraded for different lengths of time in Emmet County, Michigan, U.S.A., *Earth Surf. Processes*, *5*, 331–345, 1980a.

Nash, D., Morphological dating of degraded normal fault scarps, *J. Geol*., *88*, 353–360, 1980b.

Press, W. H., B. P. Flannery, S. A. Teukolsky, and W. T. Vetterling, *Numerical Recipes*, Cambridge Univ. Press, New York, 1986.

Roering, J. J., J. W. Kirchner, and W. E. Dietrich, Evidence for nonlinear, diffusive sediment transport on hillslopes and implications for landscape morphology, *Water Resour. Res*., *35*, 853–870, 1999.

Sklar, L., and W. E. Dietrich, River longitudinal profiles and bedrock incision models: Stream power and the influence of sediment supply, in *Rivers Over Rock: Fluvial Processes in Bedrock Channels*, edited by K. J. Tinkle and E. E. Wohl, *Geophys. Monogr. Ser*., vol. 107, pp. 237–260, AGU, Washington, D. C., 1998.

S. Fagherazzi, School of Computational Science and Information Technology, Florida State University, Tallahassee, FL 32306-4120. (sergio@csit.fsu.edu)

D. J. Furbish, Department of Geological Sciences, Florida State University, Tallahassee, FL 32306-4100. (dfurbish@garnet.acns.fsu.edu)

(Received February 18, 2000; revised January 29, 2001;
accepted March 27, 2001.)